

## Dimeric and Monomeric *Bacillus subtilis* RNase P Holoenzyme in the Absence and Presence of Pre-tRNA Substrates<sup>†</sup>

Alessandra Barrera,<sup>‡,§</sup> Xingwang Fang,<sup>‡,§,||</sup> Jaby Jacob,<sup>‡,⊥</sup> Elizabeth Casey,<sup>‡</sup> P. Thiagarajan,<sup>⊥</sup> and Tao Pan<sup>\*,‡</sup>

Department of Biochemistry and Molecular Biology, University of Chicago, 920 East 58th Street, Chicago, Illinois 60637, and Argonne National Laboratory, 9700 South Cass Avenue, Argonne, Illinois 60439

Received June 13, 2002; Revised Manuscript Received August 14, 2002

**ABSTRACT:** Ribonuclease P (RNase P) is a ribonucleoprotein enzyme that catalyzes the 5' maturation of tRNA precursors. The bacterial RNase P holoenzyme is composed of a large, catalytic RNA and a small protein. Our previous work showed that *Bacillus subtilis* RNase P forms a specific "dimer" that contains two RNase P RNA and two RNase P protein subunits in the absence of substrate. We investigated the equilibrium and the structure of the dimeric and the monomeric holoenzyme in the absence and presence of substrates by synchrotron small-angle X-ray scattering, 3' autolytic processing, and hydroxyl radical protection. In the absence of substrate, the dimer–monomer equilibrium is sensitive to monovalent ions and the total holoenzyme concentration. At 0.1 M NH<sub>4</sub>Cl, formation of the dimer is strongly favored, whereas at 0.8 M NH<sub>4</sub>Cl, the holoenzyme is a monomer. Primary hydroxyl radical protection in the dimer is located in the specificity domain, or domain I, of the RNase P RNA. The ES complex with a substrate containing a single tRNA is always monomeric. In contrast, the dominant ES complex with a substrate containing two tRNAs is dimeric at 0.1 M NH<sub>4</sub>Cl and monomeric at 0.8 M NH<sub>4</sub>Cl. Our results show that the *B. subtilis* holoenzyme can be a dimer and a monomer, and the fraction of the dimer is very sensitive to the environment. Under a variety of conditions, both the holoenzyme dimer and monomer can be present in significant amounts. Because the majority of tRNA genes are organized in large operons and because of the lack of RNase E in *B. subtilis*, a dimeric holoenzyme may be necessary to facilitate the processing of large precursor tRNA transcripts. Alternatively, the presence of two forms of the RNase P holoenzyme may be required for other yet unknown functions.

RNase P is a ribonucleoprotein enzyme that catalyzes the formation of the mature 5' end of all tRNAs through a site specific endonucleolytic cleavage reaction (1, 2). The bacterial RNase P is composed of a large RNA of ~300–400 nucleotides and a small protein of ~120 amino acids. Because the bacterial RNase P RNA<sup>1</sup> alone is catalytically active, a large body of work has been carried out in an effort to understand how this ribozyme performs this catalytic reaction (reviewed in refs 1–3). More recent studies have focused on the function and structure of the bacterial RNase P protein (4–20). A principal functional role of the protein is the enhancement of substrate binding (8, 10, 11).

We have shown previously that in contrast to the earlier assumptions, the *Bacillus subtilis* RNase P holoenzyme contains two RNase P RNA (P RNA) and two RNase P

protein (P protein) subunits under the same conditions as previous biochemical studies of the *B. subtilis* RNase P (17). The holoenzyme dimer is completely mediated by the P protein, and the RNase P RNA alone is always a monomer. The specificity of the RNase P dimer is "topological" and not based on the affinity of the binding of P protein to P RNA. Even though the *Escherichia coli* RNase P RNA (M1 RNA) binds equally well to the *B. subtilis* RNase P protein, the P RNA–P protein complex and the M1 RNA–P protein complex form a mixture of aggregates, not a specific dimer. Because the holoenzyme dimer is nearly as compact as the monomeric P RNA, small-angle X-ray scattering (SAXS) is used in the previous and in this work to determine the oligomerization state of the holoenzyme. Unlike size-exclusion and gel shift methods, the size (the scattering at zero angle, *I*<sub>0</sub>) and the shape (the radius of gyration, *R*<sub>g</sub>) of the complex are measured independently in SAXS.

Finding the RNase P dimer in vitro suggests the possibility that two ribonucleoprotein complexes may exist in the cell: one containing two P RNA and two P protein subunits (henceforth termed a holoenzyme dimer) and another containing one P RNA and one P protein subunit (henceforth termed a holoenzyme monomer). The possible existence of two oligomeric states of a bacterial RNase P also implies that multiple enzyme–substrate complexes may form to facilitate pre-tRNA processing or even to perform other yet unknown functions.

The relatively small *B. subtilis* P protein contains three potential RNA binding surfaces (9). One of the three binding

<sup>†</sup> Supported by Grant GM52993 from the National Institutes of Health. This work benefited from a grant (99-8327) to P.T. from the Packard Foundation Interdisciplinary Science program and the facilities of BESSRC-CAT and IPNS funded by the U.S. Department of Energy under Contract W31-109-ENG-38 to the University of Chicago (Chicago, IL).

\* To whom correspondence should be addressed. Phone: (773) 702-4179. Fax: (773) 702-0439. E-mail: taopan@midway.uchicago.edu.

<sup>‡</sup> University of Chicago.

<sup>§</sup> These authors contributed equally to this work.

<sup>||</sup> Present address: Ambion, Inc., 2130 Woodward St., Austin, TX 78744.

<sup>⊥</sup> Argonne National Laboratory.

<sup>1</sup> Abbreviations: *K*<sub>D</sub>, apparent dimerization constant; P RNA, RNA subunit of the *B. subtilis* RNase P; P protein, protein subunit of the *B. subtilis* RNase P; SAXS, small-angle X-ray scattering.

sites directly contacts the 5' leader of a pre-tRNA substrate, whereas the two other sites are thought to contact the P RNA. The *B. subtilis* P RNA is made of two domains; the catalytic domain contains the entire active site, and the specificity domain binds the T stem-loop portion of a tRNA (21–23). In our previously proposed symmetrical arrangement of the holoenzyme dimer, a P RNA binding site on one P protein binds to one domain on a P RNA and another P RNA binding site on this same protein binds to the other domain on the other P RNA subunit. Because the holoenzyme dimer is very compact, additional RNA–RNA interactions among the two P RNA subunits are also likely.

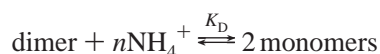
This work demonstrates that the dimeric and monomeric forms of the *B. subtilis* RNase P holoenzyme are in equilibrium, in the absence and presence of substrates. The fraction of the holoenzyme dimer and the holoenzyme monomer is very sensitive to the monovalent salt concentration. Upon binding to a substrate containing a single tRNA, the ES complex is primarily in the monomeric form. Upon binding to a substrate containing two tRNAs, however, most ES complexes can be in the dimeric form. The specificity domain of the P RNA is primarily responsible for the dimerization of the holoenzyme. We propose a model in which the *B. subtilis* RNase P holoenzyme dimer is needed to facilitate processing of large tRNA precursors.

## MATERIALS AND METHODS

**Preparation of RNAs and the P Protein.** RNAs were obtained by in vitro transcription using T7 RNA polymerase and the standard protocol (24). The transcription template for the pre-tRNA substrate containing two tRNAs was generated by PCR amplification using the genomic DNA of the *B. subtilis* (strain ATCC 6333). The PCR product was then cloned into the *Sma*I site of a pUC18 plasmid. The P protein was prepared from an overexpression clone as described previously (12). The concentration of all RNAs was obtained by the absorbance at 260 nm in 50 mM NH<sub>4</sub>-OAc as described previously (17).

**Small-Angle X-ray Scattering.** SAXS experiments were carried out at the SAXS instrument on the BESSRC ID-12 beamline at the Advanced Photon Source, Argonne National Laboratory (25). Sample handling and data processing were identical to those described previously (17). All experiments were carried out with 2.4 μM total P RNA and 2.4 μM total P protein. The NH<sub>4</sub>Cl titrations for the holoenzyme alone were performed in 20 mM Bistris-HCl (pH 6.5), 10 mM MgCl<sub>2</sub>, and 0.1–0.8 M NH<sub>4</sub>Cl using a 5 M NH<sub>4</sub>Cl stock. The substrate titrations were performed in 20 mM Bistris-HCl (pH 6.5), 10 mM CaCl<sub>2</sub>, and 0.1 or 0.8 M NH<sub>4</sub>Cl. The substitution of MgCl<sub>2</sub> with CaCl<sub>2</sub> at pH 6.5 sufficiently decreased the cleavage rate so that only an insignificant amount of substrate was cleaved during the SAXS experiment (data not shown).

The NH<sub>4</sub>Cl dependence of the dimer–monomer equilibrium was analyzed according to



where the apparent dimerization constant ( $K_D$ , in micromolar) is defined as

$$K_D = [\text{monomer}]^2/[\text{dimer}] = K[\text{NH}_4^+]^n \quad (1a)$$

The weight fraction of the dimer ( $f_D$ ) equals

$$f_D = (4C_t + K_D - \sqrt{K_D^2 + 8K_D C_t})/4C_t \quad (1b)$$

where  $C_t$  is the total concentration of the P RNA–P protein complex, i.e., 2.4 μM in our experiments. For the SAXS measurements, the  $I_0$  value is proportional to the weight concentration times the molecular mass; hence,  $I_0^{\text{dimer}} = 2I_0^{\text{monomer}}$ , and the experimental  $I_0$  value is expressed as

$$I_0 = f_M I_0^{\text{monomer}} + f_D I_0^{\text{dimer}} = (1 + f_D) I_0^{\text{monomer}} \quad (1c)$$

Combining eqs 1a–c, we obtain

$$I_0 = [1 + (4C_t + K_D - \sqrt{K_D^2 + 8K_D C_t})/4C_t] I_0^{\text{monomer}} \quad (2)$$

where  $K_D$  depends on the NH<sub>4</sub>Cl concentration and is equal to  $K_D(0.1)([\text{NH}_4^+]/0.1)^n$ . Once the experimental data are fit, two useful parameters can be obtained: the dimerization constant at 0.1 M NH<sub>4</sub>Cl [ $K_D(0.1)$ ] and the ionic dependence of the dimerization constant ( $n$ ).

**Hydroxyl Radical Protection.** Hydroxyl radical protection was carried out using the standard Fe(II)–EDTA method in 20 mM Tris-HCl (pH 7.5), 10 mM MgCl<sub>2</sub>, 0.1–0.8 M NH<sub>4</sub>-Cl, 2.4 μM P RNA, and 2.4 μM P protein at 37 °C (21, 26). To reconstitute the holoenzyme, P RNA alone in buffer was heated at 85 °C for 2 min, followed by incubation for 3 min at room temperature. MgCl<sub>2</sub> was added, and the mixture was incubated for 3 min at 50 °C. An equimolar ratio of P protein was added, followed by the addition of NH<sub>4</sub>Cl at the designated concentrations. This mixture was further incubated for 5 min at 37 °C. Ascorbic acid and dithiothreitol were added to final concentrations of 1 and 5 mM, respectively. The reaction was immediately initiated by adding 1 mM Fe(II) and 1.2 mM EDTA and allowed to proceed for 30 min at 37 °C. The reaction was quenched upon addition of 10 mM thiourea. The mixture was then separated on polyacrylamide gels containing 7 M urea, and the cleavage products were quantitated by phosphorimaging.

The term “protection factor” was used to quantify the extent of protection of individual residues due to dimerization (21). The protection factor is defined as the amount of radioactivity in each band at 0.7 M NH<sub>4</sub>Cl divided by that of the same band at 0.1 M NH<sub>4</sub>Cl. This number is then normalized to the amount of radioactivity of the cleaved products in each lane. In principle, a protection factor of >1.0 would indicate protection against hydroxyl radical cleavage when comparing these two conditions. In this work, a protection factor of >1.5 is considered to fully represent protection upon dimerization.

**Autolytic Processing of the 3' End.** The 3' <sup>32</sup>P-labeled P RNA precursors (Figure 1A, left) were first renatured as described above at the designated NH<sub>4</sub>Cl concentration. The reaction was initiated at 37 °C upon addition of the P protein in equimolar ratios. The final reaction mixture contained 20 mM Tris-HCl (pH 7.5), 10 mM MgCl<sub>2</sub>, and 0.1–0.8 M NH<sub>4</sub>-Cl. Aliquots at designated time points were mixed with an excess of 9 M urea and 100 mM EDTA to stop the reaction. The mixture was then analyzed on denaturing polyacrylamide gels containing 7 M urea. The amounts of products and substrates were quantitated by phosphorimaging.

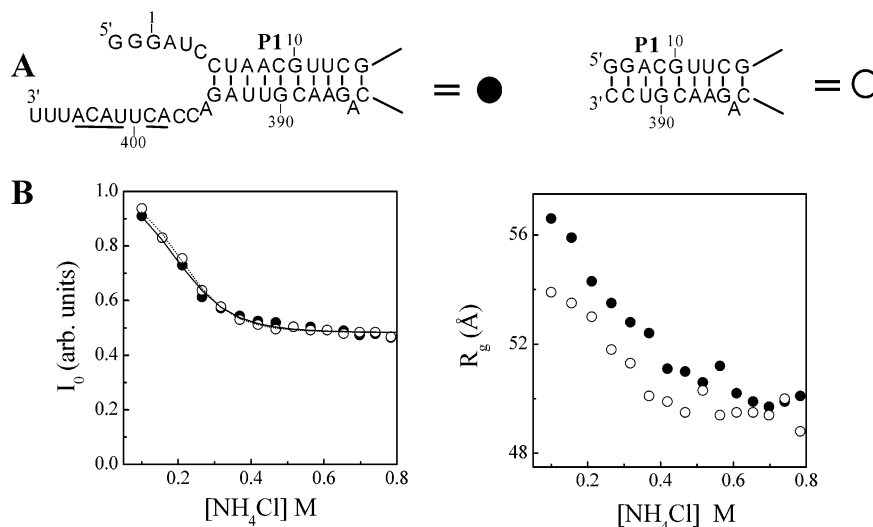


FIGURE 1: (A) Sequence of the terminal regions of the two P RNA constructs used in the SAXS study. The 3' autolytic processing sites are underlined (15). (B) Small-angle X-ray scattering of the *B. subtilis* RNase P holoenzyme at 2.4  $\mu\text{M}$  total P RNA and 2.4  $\mu\text{M}$  total P protein in 20 mM Bistris-HCl (pH 6.5) and 10 mM  $\text{MgCl}_2$  at 37 °C. The  $\text{NH}_4\text{Cl}$  concentration was varied from 0.1 to 0.8 M. On the left, the  $I_0$  value at 0.1 M  $\text{NH}_4\text{Cl}$  is 2 times the value at 0.8 M. The salt dependence of dimerization is fit to eq 2. At the right, the  $R_g$  values of the holoenzyme dimer (0.1 M  $\text{NH}_4\text{Cl}$ ) and the monomer are  $\sim 57$  and  $\sim 50$  Å, respectively.

**Activity Assays.** All reactions were performed under single-turnover conditions at 2.4  $\mu\text{M}$  holoenzyme and  $< 2$  nM 5' or 3'  $^{32}\text{P}$ -labeled pre-tRNA substrates. The holoenzyme was reconstituted as described above at 50 mM MES (pH 5.8), 10 mM  $\text{MgCl}_2$ , and 0.1 or 0.8 M  $\text{NH}_4\text{Cl}$ . The pre-tRNA substrates were renatured by heating in the buffer alone at 85 °C for 2 min and at room temperature for 3 min, addition of  $\text{MgCl}_2$ , incubation at 37 °C for 5 min, and finally addition of  $\text{NH}_4\text{Cl}$ . The cleavage reaction was initiated upon mixing an equal volume of the renatured holoenzyme and the substrate. Aliquots were taken at the designated time points and mixed with an excess of 9 M urea and 100 mM EDTA to stop the reaction. The reaction products were separated from the unreacted substrates on denaturing gels containing 7 M urea. The amounts of products and substrates were determined by phosphorimaging.

## RESULTS

**Holoenzyme Dimer–Monomer Equilibrium.** The fraction of the holoenzyme dimer and monomer as a function of monovalent salt concentration is determined by synchrotron small-angle X-ray scattering (SAXS, Figure 1B). Two SAXS-derived parameters are used to deduce the fraction of the dimer and the monomer, the scattering intensity at zero angle ( $I_0$ ), and the change in the radius of gyration ( $R_g$ ). Because the P protein scatters only one-fifth as intensely as P RNA and it weighs only one-tenth as much as P RNA,  $I_0$  is directly proportional to the molecular mass of the P RNA in the complex. At 0.8 M  $\text{NH}_4\text{Cl}$ ,  $I_0$  is nearly 2-fold less than  $I_0$  at 0.1 M  $\text{NH}_4\text{Cl}$ . The  $R_g$  value for the complex is also reduced from  $\sim 57$  Å at 0.1 M  $\text{NH}_4\text{Cl}$  to  $\sim 50$  Å at 0.8 M  $\text{NH}_4\text{Cl}$ . These results show that at 2.4  $\mu\text{M}$  holoenzyme, nearly all complexes are dimers at 0.1 M  $\text{NH}_4\text{Cl}$  and nearly all complexes are monomers at 0.8 M  $\text{NH}_4\text{Cl}$ . At the intermediate  $\text{NH}_4\text{Cl}$  concentration, the holoenzyme is in the dimer–monomer equilibrium.

A fit of the SAXS result by eq 2 shows that the dimer–monomer equilibrium has a fifth-power dependence on the  $\text{NH}_4\text{Cl}$  concentration; i.e., the dimerization constant,  $K_D$ , is

reduced by  $2^5$ -fold when the  $\text{NH}_4\text{Cl}$  concentration is increased by 2-fold. The  $K_D$  value at 0.1 M  $\text{NH}_4\text{Cl}$  extrapolated from the SAXS data is  $\sim 50$  nM. The dimerization constant is similar to that of binding of the RNase P protein alone to other unrelated RNAs, e.g., the *Tetrahymena* group I ribozyme (17) or the 5S rRNA (27). As we have demonstrated in the previous work, the specificity of the RNase P dimer is “topologically specific”, not simply based on the affinity of binding of P protein to P RNA.

The same dimer–monomer equilibrium is observed when the 5' or 3' single-stranded regions in the P RNA are deleted (Figure 1). This result suggests that dimerization of the holoenzyme is not due to the P protein binding to these single-stranded regions in the P RNA.

A second, independent assay is performed to evaluate the dimer–monomer equilibrium (Figure 2). The *B. subtilis* holoenzyme undergoes autolytic processing at its 3' end in vitro (15). The autolytic processing reaction is also sensitive to the  $\text{NH}_4\text{Cl}$  concentration. An overlay of the processing rate with the SAXS data indicates that this processing reaction quantitatively reproduces the monovalent ion dependence of the holoenzyme dimerization (Figure 2C). Therefore, the 3' autolytic processing is carried out exclusively by the holoenzyme dimer.

The conclusion of 3' autolytic processing as the exclusive property of the holoenzyme dimer is further supported by the following results. (i) When the total concentration of the holoenzyme is decreased by  $\sim 50$ -fold to 50 nM, which is the middle point concentration for the holoenzyme dimerization, the autolytic processing rate decreases by only  $\sim 2$ -fold (Figure 2B). (ii) A single-stranded RNA containing the same sequence as nucleotides 392–402 of the P RNA is not cleaved under the same condition used for autolytic processing (data not shown). (iii) We have demonstrated previously that the *B. subtilis* holoenzyme is an active endonuclease for several single-stranded RNAs (15). The autolytic processing rate at 0.1  $\mu\text{M}$  holoenzyme, however, is at least 10-fold faster than the cleavage of the best single-stranded RNA substrate used in that study.



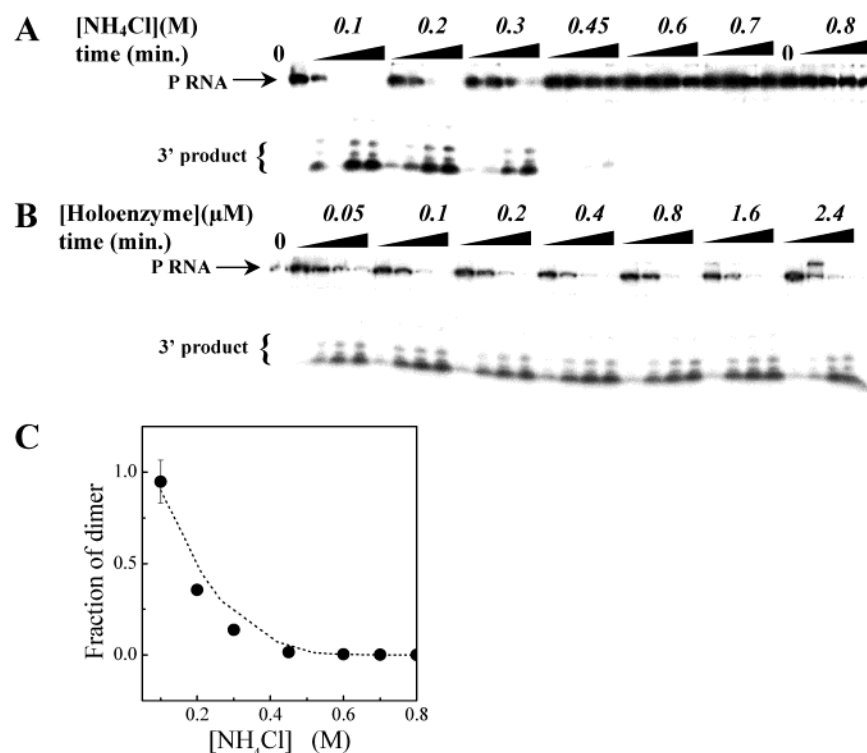


FIGURE 2: Autolytic processing of the *B. subtilis* holoenzyme using 3'-labeled P RNA at 37 °C. (A) Processing is significantly faster at lower NH<sub>4</sub>Cl concentrations. The reaction mixture also contains 20 mM Tris-HCl (pH 7.5) and 10 mM MgCl<sub>2</sub>. (B) Processing is not very sensitive to the total holoenzyme concentration, consistent with the notion that autolytic processing primarily occurs within the dimer. (C) Overlay of the autolytic processing rate (●) with the dimer fraction determined by SAXS (---).

Because the autolytic processing occurs in *cis*, i.e., by the holoenzyme dimer alone, a simple model would place the 3' end of one P RNA subunit close to the active site of the other P RNA subunit in the holoenzyme dimer. Alternatively, a large-scale conformational change occurs during the processing reaction. Regardless, the combined results from SAXS and autolytic processing clearly demonstrate that the holoenzyme can be present in the dimeric and in the monomeric form. The precise fraction of these two forms is very sensitive to the solution condition, in particular, the monovalent ion concentration.

**Hydroxyl Radical Protection of the Holoenzyme Dimer and Monomer.** To reveal the molecular details of the holoenzyme structure, hydroxyl radical protection is carried out under ionic concentrations identical to those in the SAXS study (Figure 3). Hydroxyl radical attacks the exposed portion of the ribose-phosphate backbone which results in strand scission. At 0.1 M NH<sub>4</sub>Cl, i.e., when the holoenzyme is nearly all in the dimeric form, many residues are protected compared to the protection pattern of the P RNA alone. In contrast, the number of protected residues is dramatically lower at 0.8 M NH<sub>4</sub>Cl, i.e., when the holoenzyme is nearly all in the monomeric form. The small number of protected regions in the monomer may be derived primarily from direct P protein contacts, an interpretation consistent with the phosphorothioate interference data (20). Most residues that are protected in the dimer but not in the monomer are located in the specificity domain of the P RNA (Figure 3B). These results show that the two domains of P RNA play distinct roles in holoenzyme assembly, where the S-domain is primarily responsible for holoenzyme dimerization.

Unexpectedly, the four protected regions in the holoenzyme dimer have two distinct sensitivities to the monovalent

salt concentration (Figure 3C). The salt dependence of regions II and III matches the dimerization property determined by SAXS. Regions I and IV are less sensitive to salt than regions II and III, suggesting that interactions involving regions I and IV may not be directly related to dimer formation. Regions II and III are located in the S-domain of the P RNA. In the folded P RNA structure in the absence of P protein, the P12 tetraloop in region III interacts with the tetraloop receptor in region II (23). The crucial role of regions II and III in the protein-mediated dimerization suggests that P protein directly binds to one of these two regions.

**Holoenzyme-Substrate Complexes.** Although the pre-tRNA substrates used in almost all biochemical studies contain a single tRNA, the cellular substrate is more diverse. The genome sequence of *B. subtilis* identifies a total of 88 tRNAs, only nine of which are present as a single tRNA transcript (28). The remaining 79 tRNAs are arranged in 13 operons ranging from 2 to 21 tRNAs per transcript. At least in *B. subtilis*, therefore, the holoenzyme is far more likely to encounter tRNA transcripts containing two or more tRNAs. For this reason, two types of substrate are chosen in this study, one containing a single tRNA substrate (pre-tRNA<sup>Phe</sup>, pre-tRNA<sup>Pro</sup>, and pre-tRNA<sup>Ala</sup>) and the other containing two tRNAs (pre-tRNA<sup>Pro</sup>-tRNA<sup>Ala</sup>). We choose to use pre-tRNA<sup>Phe</sup> for the SAXS study because this substrate has been extensively studied in our laboratory and the results can be compared to our previous work.

Substrate binding of the holoenzyme is examined by SAXS (Figure 4) and by the activity assay under single-turnover conditions (Table 1). To avoid significant cleavage during the SAXS experiments, MgCl<sub>2</sub> was substituted with CaCl<sub>2</sub> and the pH was decreased to 6.5. The *I*<sub>0</sub> value can again be used to quantitatively analyze the formation of

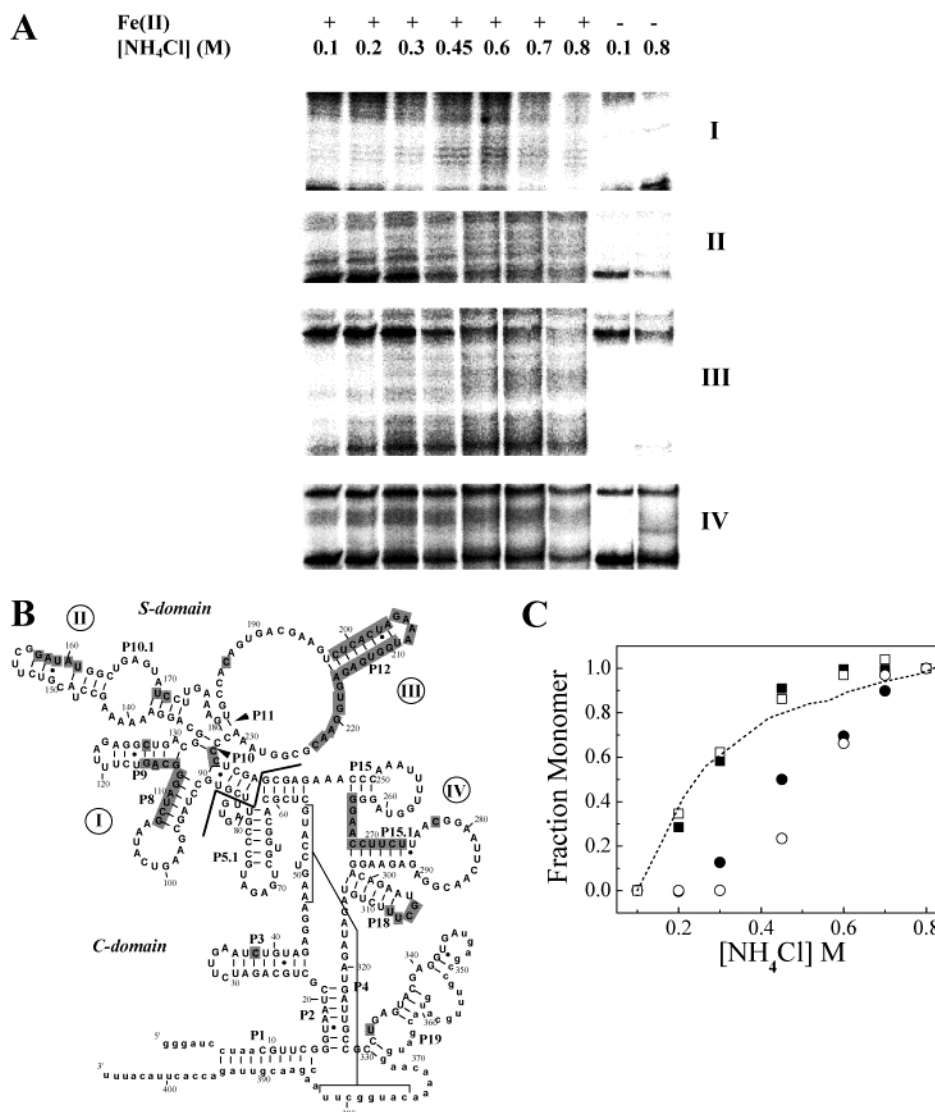


FIGURE 3: Hydroxyl radical protection of the holoenzyme as a function of  $\text{NH}_4\text{Cl}$  concentration. The conditions are chosen according to the SAXS data shown in Figure 1, where the holoenzyme is a dimer at 0.1 M  $\text{NH}_4\text{Cl}$  and a monomer at 0.8 M  $\text{NH}_4\text{Cl}$ . (A) Four regions showing significant changes in the protection pattern. Hydroxyl radical cleavage at high  $\text{NH}_4\text{Cl}$  concentrations is slower so that the amount of radioactivity of all cleavage bands decreases at 0.7 and 0.8 M  $\text{NH}_4\text{Cl}$ . The loss of protection at high  $\text{NH}_4\text{Cl}$  concentrations is readily apparent upon normalization of the cleaved bands in these regions against cleavage products not protected in the presence of the P protein. (B) Summary of the protection comparing the holoenzyme dimer (0.1 M  $\text{NH}_4\text{Cl}$ ) and monomer (0.7 M  $\text{NH}_4\text{Cl}$ ). Residues that have protection factors of  $>1.5$  are shaded. Residues in lowercase letters could not be analyzed due to the resolution of gel electrophoresis. The specificity domain (S-domain) is composed of residues 86–239. (C) Salt dependence of regions I (●), II (■), III (□), and IV (○). The SAXS data from Figure 1B are shown as a dashed line.

monomeric and dimeric complexes, whereas the  $R_g$  value provides information about the structure of the complexes. Upon substrate addition and complex formation, the  $I_0$  value is proportional to the second power of the molecular mass ratio of the ES complex and the holoenzyme alone:

$$I_0^{\text{ES}}/I_0^{\text{E}} = (\text{MW}^{\text{ES}}/\text{MW}^{\text{E}})^2 \quad (3)$$

The precision of the quantitative assessment of monomeric–dimeric ES complexes is hindered by the inaccuracy in the determination of RNA concentrations and by the fraction of ribozyme and substrates that are properly folded. Using an empirical factor derived from the experimental results that includes both concentration difference and folding defect can, however, correct for these effects (Figure 4 and Table 1). This factor is  $\sim 0.83$  for the experiments with pre-tRNA<sup>Phe</sup> and  $\sim 0.60$  for the experiments with pre-tRNA<sup>Pro</sup>–tRNA<sup>Ala</sup>.

The formation of the holoenzyme–substrate complex is monitored at 0.1 and 0.8 M  $\text{NH}_4\text{Cl}$  as the molar E:S ratio is varied from 0 to 2 (Figure 4). The holoenzyme concentration is kept at  $2.4 \mu\text{M}$  to ensure that the initial holoenzyme is a dimer, i.e., at 0.1 M  $\text{NH}_4\text{Cl}$ , or a monomer, i.e., 0.8 M  $\text{NH}_4\text{Cl}$ . Under our conditions, the affinity of P RNA for a tRNA substrate is high enough that all properly folded substrates are bound to the P RNA when the substrate:ribozyme stoichiometry is less than 1.

When the holoenzyme is initially a dimer, i.e., at 0.1 M  $\text{NH}_4\text{Cl}$ , the  $I_0$  value decreases upon addition of pre-tRNA<sup>Phe</sup> until the molar ratio of the substrate to the total RNase P holoenzyme concentration is  $\sim 1$  [Figure 4A (●)]. Further addition of pre-tRNA<sup>Phe</sup> produces only a very slight increase in the  $I_0$  value for which the presence of uncomplexed pre-tRNA<sup>Phe</sup> accounts. When the holoenzyme is initially a monomer, i.e., at 0.8 M  $\text{NH}_4\text{Cl}$ , the  $I_0$  value increases upon

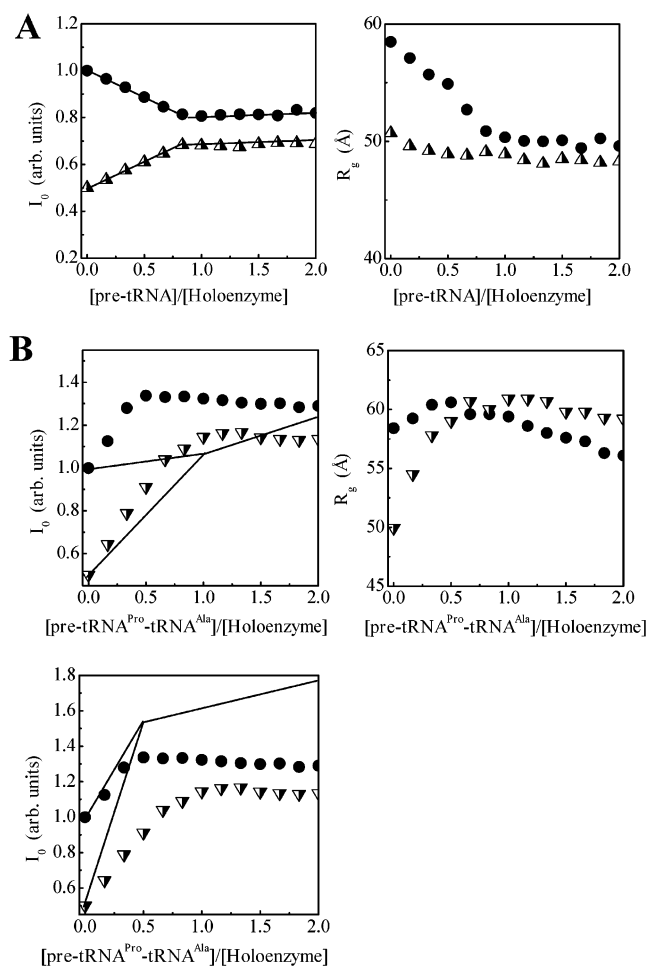


FIGURE 4: Small-angle X-ray scattering of the ES complexes at 37 °C. All mixtures contain 2.4  $\mu$ M total P RNA and 2.4  $\mu$ M total P protein in 20 mM Bistris-HCl (pH 6.5) and 10 mM  $\text{CaCl}_2$ . (A) ES complex upon addition of pre-tRNA<sup>Phe</sup> at 0.1 (●) and 0.8 M  $\text{NH}_4\text{Cl}$  (▲). Lines show the complex formation using a correction factor of 0.83, derived from the uncertainties in RNA concentration and/or misfolding of a small fraction of either RNA. Only the monomeric ES complex forms with this substrate containing a single tRNA. (B) ES complex upon addition of the pre-tRNA<sup>Pro</sup>–tRNA<sup>Ala</sup> substrate at 0.1 (●) and 0.8 M  $\text{NH}_4\text{Cl}$  (▼). In the  $I_0$  graphs, lines represent the calculated values for two extreme cases: (top) all ES complexes contain one holoenzyme subunit ( $\text{ES}_{\text{monomer}}$ ), and (bottom) all ES complexes contain two holoenzyme subunits ( $\text{ES}_{\text{dimer}}$ ).

addition of pre-tRNA<sup>Phe</sup> until the molar ratio of the substrate to the total P RNA concentration is  $\sim 1$  [Figure 4A (▲)]. These results show that the ES complex containing a single pre-tRNA substrate is a monomer. Binding of a single tRNA substrate appears to compete with dimer formation, potentially due to the overlap of the substrate binding site with the RNA–protein or RNA–RNA interactions in the holoenzyme dimer in the absence of substrate.

Different ES complexes are observed when the substrate containing two tRNAs, pre-tRNA<sup>Pro</sup>–tRNA<sup>Ala</sup>, is bound to the holoenzyme (Figure 4B). The three lines represent two extreme cases where the ES complex is either completely monomeric (top panel) or completely dimeric (bottom panel). Unlike the results with the pre-tRNA<sup>Phe</sup> substrate, both substrate titrations at 0.1 and 0.8 M  $\text{NH}_4\text{Cl}$  do not show such extreme behavior.

The ES complex is almost exclusively a dimer at 0.1 M  $\text{NH}_4\text{Cl}$  when the holoenzyme is in molar excess over the

substrate, taking into account the fact that only  $\sim 60\%$  of this substrate is properly folded. Upon addition of more substrates, the monomeric ES complex forms, presumably due to holoenzyme binding to one tRNA in pre-tRNA<sup>Pro</sup>–tRNA<sup>Ala</sup>. Addition of excess substrate results in the formation of more monomeric ES complex. The system is now in the monomer–dimer equilibrium. Both monomeric and dimeric ES complexes still form at 0.8 M  $\text{NH}_4\text{Cl}$ , but the fraction of the dimeric complex is significantly lower. Without further analysis, it is unclear whether the dimeric ES complexes at 0.1 and 0.8 M  $\text{NH}_4\text{Cl}$  have the same structure. Regardless, the presence of two ES complexes appears to be ubiquitous under vastly different conditions.

The cleavage reaction under single-turnover conditions shows some unexpected results (Figure 5 and Table 1). For the pre-tRNA<sup>Pro</sup> and pre-tRNA<sup>Ala</sup> substrates that contain only a single tRNA, the cleavage rate for a fraction of the substrate is essentially identical to those obtained by cleavage of a pre-tRNA<sup>Asp</sup> substrate upon adjustment of the pH (8). The remaining substrate is cleaved at a much slower rate. When these two tRNAs are linked into the pre-tRNA<sup>Pro</sup>–tRNA<sup>Ala</sup> substrate, two cleavage reactions occur (Figure 5B). Cleavage of the first tRNA has the same rate as cleavage of the single pre-tRNA substrates. Therefore, the first cleavage of this two-tRNA substrate likely occurs randomly. However, subsequent cleavage of the second tRNA substrate is at least 2-fold slower than the first cleavage.

A trivial explanation for the slower rate of the second cleavage reaction is that the first reaction cleaves the properly folded substrate fraction, whereas the second reaction corresponds to the cleavage of the improperly folded substrate. A second explanation for the slower cleavage rate is that the first cleavage generates a product that contains a 3' tail (in the case of  $k_3^{\text{obs}}$ ) or a 5' tRNA (in the case of  $k_4^{\text{obs}}$ ). These extra pieces of RNA somehow interfere with the second cleavage. A third, more interesting scenario is that the slower cleavage of the second tRNA may be relevant for a possible function of the holoenzyme dimer. As discussed below, processive processing of large tRNA precursors by the *B. subtilis* RNase P may be required in vivo.

## DISCUSSION

*Dimer versus Monomer or Dimer plus Monomer?* We demonstrate in this work that the *B. subtilis* RNase holoenzyme can exist as a dimer and as a monomer. The fraction of each form depends on many factors, including the monovalent ion concentration, the total holoenzyme concentration, and the presence of substrates. These observations inevitably raise two significant questions. Is the holoenzyme a dimer or a monomer in the cell? What are the potential functions of the dimer and/or the monomer?

As far as we are aware, there is currently no simple way of distinguishing a 250 kDa dimer and a 125 kDa monomer in a *living* bacterial cell. If it is assumed that such a technique is available, the measurements still may not be conclusive because either of the two oligomers may exist only transiently, thereby remaining undetectable in a static state. *B. subtilis* was estimated to contain 20–50 RNase P molecules per cell (29). If a uniform distribution of these molecules is assumed, the total concentration of the RNase P is 17–42 nM. *B. subtilis*, however, is known to have separate compart-

Table 1: Cleavage Rates (in  $s^{-1}$ ) of Substrates Containing One or Two tRNAs at 37 °C

substrate <sup>a</sup>	$k_1^{obs}$ , $k_2^{obs}$	fraction cleaved	$k_3^{obs}$ , $k_4^{obs}$	fraction cleaved
pre-tRNA <sup>Pro</sup> —tRNA <sup>Ala</sup>				
0.1 M NH <sub>4</sub> Cl	$0.10 \pm 0.01^b$ , $0.14 \pm 0.01^c$	$0.63 \pm 0.01$ , $0.91 \pm 0.01$	$<0.002^b$ , $0.08 \pm 0.01^c$	$<0.01$ , $0.31 \pm 0.03$
0.8 M NH <sub>4</sub> Cl	$0.17 \pm 0.01^b$ , $0.12 \pm 0.02^c$	$0.87 \pm 0.01$ , $0.75 \pm 0.03$	$0.05 \pm 0.01^b$ , $0.05 \pm 0.02^c$	$0.08 \pm 0.01$ , $0.17 \pm 0.06$
pre-tRNA <sup>Pro</sup>				
0.1 M NH <sub>4</sub> Cl	$0.13 \pm 0.01$	$0.50 \pm 0.02$		
0.8 M NH <sub>4</sub> Cl	$0.17 \pm 0.03$	$0.51 \pm 0.02$		
pre-tRNA <sup>Ala</sup>				
0.1 M NH <sub>4</sub> Cl	$0.14 \pm 0.02$	$0.84 \pm 0.02$		
0.8 M NH <sub>4</sub> Cl	$0.17 \pm 0.02$	$0.80 \pm 0.02$		

<sup>a</sup> All reaction mixtures contained 50 mM MES (pH 5.8) and 10 mM MgCl<sub>2</sub>. The cleavage rate for the pre-tRNA<sup>Phe</sup> substrate is  $0.14 \pm 0.04 s^{-1}$  under this condition with 0.1 M NH<sub>4</sub>Cl. <sup>b</sup>  $k_1^{obs}$  and  $k_3^{obs}$  are obtained from 5'-labeled substrate. <sup>c</sup>  $k_2^{obs}$  and  $k_4^{obs}$  are obtained from 3' labeled substrate.

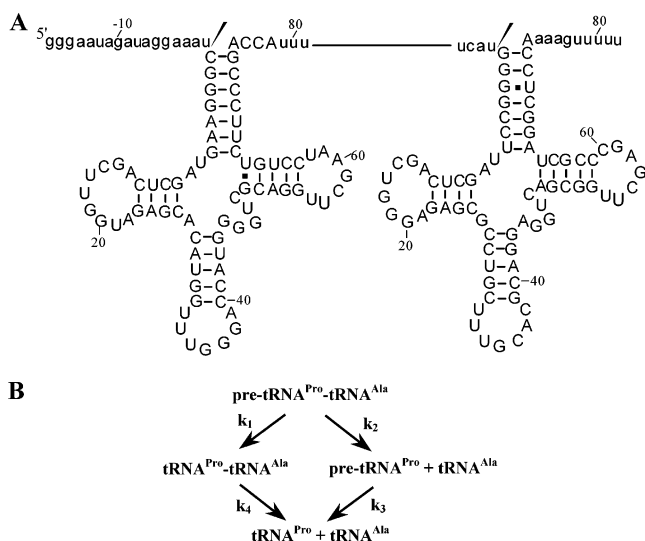


FIGURE 5: (A) Sequence and proposed secondary structure of the two-tRNA substrate (pre-tRNA<sup>Pro</sup>—tRNA<sup>Ala</sup>). The cleavage sites are denoted with two daggers. (B) Reaction scheme for cleaving the pre-tRNA<sup>Pro</sup>—tRNA<sup>Ala</sup> substrate.

ments for transcription and translation (30). Therefore, the intracellular local concentration of RNase P is likely to be higher. Even at the lower estimate of the RNase P concentration, the fraction of the dimer is approximately 30% using the  $K_D$  determined at 0.1 M NH<sub>4</sub>Cl. On the basis of these calculations, it is probably safe to assume that both the dimer and monomer exist in *B. subtilis*.

Because the dimer and monomer can process substrates equally well, the oligomerization state probably does not matter in the processing of substrates containing one or two tRNAs. On the other hand, the presence of two substrate binding sites in a dimer creates the possibility of processive tRNA processing for substrates that contain many more tRNAs. The largest tRNA operon in *B. subtilis* contains 21 tRNAs, and it is conceivable that processive processing of such a gigantic substrate would be advantageous. It is not yet possible to demonstrate the potential processivity of tRNA processing due to severe problems in misfolding of in vitro transcripts containing more than two tRNAs (A. Loria and T. Pan, unpublished results).

An often-neglected suggestion is that tRNA processing may occur differently in *B. subtilis* and in *E. coli*. First, 76% of all tRNAs in *B. subtilis* are arranged in operons with more than four tRNAs, compared to only 31% of all tRNAs in *E. coli*. Second, the tRNA operons in *B. subtilis* contain up to 21 tRNAs, compared to just seven tRNAs in *E. coli*. Third, transcripts containing several tRNAs in *E. coli* are cleaved

first by RNase E to generate substrates that contain only one or two tRNAs for the *E. coli* RNase P (31, 32). An RNase E homologue, however, has not been found in *B. subtilis*, so the *B. subtilis* RNase P may have become more efficient in processing substrates containing multiple tRNAs. To our knowledge, no definitive studies have been published to show whether *E. coli* RNase P is a monomer or a dimer. The oligomerization state and the associated functions of *E. coli* RNase P remain an open question.

**Structure of the Holoenzyme Dimer and Monomer and the ES Complexes.** The structural arrangement of the two P RNA subunits in the holoenzyme dimer has been modeled to be symmetrical in our previous work (17). In that model, the S-domain of one P RNA subunit is proximal to the C-domain of the other subunit. In a symmetrical arrangement involving two P proteins, one of the P protein sites would contact one P RNA while another P protein site would contact the other P RNA subunit. In the dimer, the P protein may contact the C-domain of one P RNA and the S-domain of the other P RNA. Due to the similar salt sensitivity, interactions involving regions II and III occur as a group and are primarily responsible for dimerization. Because the P protein mediates dimerization, a strong candidate for direct protein–RNA interaction is region III that contains both nonhelical (J12/11) and helical (P12) structures.

The dimer formation initiated by P protein binding brings the two P RNA subunits into proximity so that RNA–RNA contacts between the two subunits can also take place. Where such RNA–RNA interactions take place is uncertain. The extensive protection in regions I and IV suggests that these regions may play a role in intersubunit RNA–RNA interaction. However, the disparity of the salt sensitivity among regions I and IV to the SAXS data makes such a suggestion less feasible. Protection involving regions I and IV may also be related to conformational issues in the holoenzyme monomer.

When a substrate containing a single tRNA binds to the holoenzyme, the ES complex is always a monomer (ES<sub>monomer</sub>). The disruption of the dimer in the ES<sub>monomer</sub> can be attributed to two effects. First, one RNA binding site on the P protein now associates with the 5' leader of the substrate. If this same binding site were also involved in dimer formation, then this rearrangement would significantly weaken the RNA–protein interactions among the subunits in the dimer. Second, the T stem–loop binding site in the S-domain becomes occupied by the substrate. This rearrangement could also reduce the strength of the RNA–RNA interactions among the subunits in the dimer.



The holoenzyme monomer can be simply modeled to have a structure similar to that of its counterpart in the dimer. The SAXS data are consistent with this model; for example, the  $R_g$  calculated from this model is  $\sim 50$  Å, similar to the experimental value. The monomer model is also consistent with the slight reduction in the  $R_g$  value upon formation of ES<sub>monomer</sub> (from 50 to 49 Å), despite the increase in the molecular mass of the complex. The  $R_g$  reduction can be considered to fill a cavity in the holoenzyme monomer by the substrate, a result not consistent with any significant change in the structure of the holoenzyme monomer upon substrate binding. In other words, the substrate binding site is likely to be preformed in the holoenzyme monomer. The same magnitude in  $R_g$  reduction is also obtained using the P RNA model proposed by Westhof and co-workers (from 43 to 42 Å).

A dimeric ES complex (ES<sub>dimer</sub>) is only formed using a substrate containing two tRNAs. There are two structural models for this dimeric ES complex. In one model, the holoenzyme dimer becomes two independent monomers upon binding of two tRNAs. The ES<sub>dimer</sub> is maintained by the covalent link between the two tRNAs in the substrate. In the other model, the holoenzyme does not become two independent monomers. Rather, some contacts between the subunits are maintained, or new contacts are formed among the subunits in ES<sub>dimer</sub>. Because the SAXS data indicate a mixture of ES<sub>dimer</sub> and ES<sub>monomer</sub>, it is difficult to distinguish these two models due to the lack of a "pure" ES<sub>dimer</sub> or ES<sub>monomer</sub> standard for the pre-tRNA<sup>Pro</sup>–tRNA<sup>Ala</sup> substrate. Given the extensive interaction between the subunits in the holoenzyme dimer in the absence of substrate, it is plausible that some contacts between the holoenzyme subunits remain in ES<sub>dimer</sub>.

**A Processive Model of *B. subtilis* RNase P Processing.** The ability of the *B. subtilis* RNase P holoenzyme to form ES<sub>dimer</sub> may be crucial in the processing of precursor tRNA substrates containing multiple tRNAs. A possible model for processive processing is discussed below, although we emphasize that vigorous experimental support for this model is still not available. In our model, the holoenzyme dimer binds to two random but adjacent tRNAs upon the initial encounter. The first cleavage reaction can occur at either the 5' or the 3' tRNA. Two reaction routes can then be used depending on whether the initial cleavage is at the 5' or 3' tRNA. (i) After the first cleavage at the 5' tRNA, the 5' holoenzyme subunit in the dimer that performed the cleavage reaction dissociates from the tRNA product and binds to the next available tRNA adjacent to the 3' holoenzyme subunit in the dimer. The second cleavage reaction is then carried out by the initial 3' subunit in the dimer. The ES complex after the second cleavage is essentially the same as the ES complex after the first cleavage, except that the substrate has become shorter by one tRNA. Cleavage continues by the alternate RNase P subunit in the dimer to progressively shorten the tRNA precursors toward the 5' end of the poly-tRNA transcript. (ii) After the first cleavage at the 3' tRNA, the 3' holoenzyme subunit in the dimer that performed the cleavage reaction dissociates from the 5' leader product and binds to the next available tRNA adjacent to the 5' holoenzyme subunit in the dimer. The second cleavage reaction is then carried out by the initial 5' subunit in the dimer. The ES complex after the second cleavage is again shorter by

one tRNA than the ES complex after the first cleavage. Cleavage continues by the alternate RNase P subunit in the dimer to progressively shorten the tRNA precursors toward the 3' end of the poly-tRNA transcript.

The processive processing model makes several predictions for holoenzyme cleavage of a multiple tRNA substrate.

(i) The first two tRNAs in the substrate bound by the holoenzyme dimer are randomly chosen, but they are always adjacent to each other to ensure interaction between the holoenzyme dimer in the substrate.

(ii) After the first cleavage, the second cleavage should take more time than the time needed for the holoenzyme to "translocate" to the adjacent tRNA in the same ES complex. This prediction is consistent with the observation that the second cleavage of the pre-tRNA<sup>Pro</sup>–tRNA<sup>Ala</sup> substrate can be significantly slower than the first cleavage (Table 1).

(iii) After the first cleavage, subsequent cleavage is unidirectional. The ES complex either cleaves only tRNAs 3' to the first cleavage site or cleaves only tRNAs 5' to the first cleavage site.

Analysis of the holoenzyme reaction with substrates containing multiple tRNAs has been technically challenging, in part due to tRNA misfolding in large multi-tRNA precursors. Screening of the folding property of multi-tRNA substrates will be necessary to allow experimental testing of the processivity model.

One shall keep in mind that the processivity model may not be applicable to all bacterial RNase P reactions. For example, the *E. coli* RNase P is unable to efficiently process multi-tRNA precursors in vivo. Rather, a 3' processing enzyme, RNase E, is the first enzyme that cleaves multi-tRNA precursors (31, 32). Interestingly, preliminary studies suggest that the *E. coli* RNase P holoenzyme has a weaker tendency to form dimers than the *B. subtilis* holoenzyme (unpublished results). Perhaps the superior ability of the *B. subtilis* holoenzyme to form dimers is simply derived from the necessity to efficiently process multi-tRNA substrates in an RNase E-minus bacterium.

## ACKNOWLEDGMENT

We thank A. Loria, other members of the Pan laboratory, and T. Sosnick for helpful discussions.

## REFERENCES

- Frank, D. N., and Pace, N. R. (1998) *Annu. Rev. Biochem.* 67, 153–180.
- Altman, S., and Kirsebom, L. (1999) in *The RNA World* (Gesteland, R. F., Cech, T. R., and Atkins, J. F., Eds.) 2nd ed., pp 351–380, Cold Spring Harbor Laboratory Press, Plainview, NY.
- Kurz, J. C., and Fierke, C. A. (2000) *Curr. Opin. Chem. Biol.* 4, 553–558.
- Talbot, S. J., and Altman, S. (1994) *Biochemistry* 33, 1399–1405.
- Talbot, S. J., and Altman, S. (1994) *Biochemistry* 33, 1406–1411.
- Gopalan, V., Golbik, R., Schreiber, G., Fersht, A. R., and Altman, S. (1997) *J. Mol. Biol.* 267, 765–769.
- Gopalan, V., Baxevanis, A. D., Landsman, D., and Altman, S. (1997) *J. Mol. Biol.* 267, 818–829.
- Kurz, J. C., Niranjanakumari, S., and Fierke, C. A. (1998) *Biochemistry* 37, 2393–2400.
- Stams, T., Niranjanakumari, S., Fierke, C. A., and Christianson, D. W. (1998) *Science* 280, 752–755.
- Crary, S. M., Niranjanakumari, S., and Fierke, C. A. (1998) *Biochemistry* 37, 9409–9416.
- Niranjanakumari, S., Stams, T., Crary, S. M., Christianson, D. W., and Fierke, C. A. (1998) *Proc. Natl. Acad. Sci. U.S.A.* 95, 15212–15217.



12. Niranjankumari, S., Kurz, J. C., and Fierke, C. A. (1998) *Nucleic Acids Res.* 26, 3090–3096.
13. Loria, A., Niranjankumari, S., Fierke, C. A., and Pan, T. (1998) *Biochemistry* 37, 15466–15473.
14. Gopalan, V., Kuhne, H., Biswas, R., Li, H., Brudvig, G. W., and Altman, S. (1999) *Biochemistry* 38, 1705–1714.
15. Loria, A., and Pan, T. (2000) *RNA* 6, 1413–1422.
16. Biswas, R., Ledman, D. W., Fox, R. O., Altman, S., and Gopalan, V. (2000) *J. Mol. Biol.* 296, 19–31.
17. Fang, X. W., Yang, X. J., Littrell, K., Niranjankumari, S., Thiagarajan, P., Fierke, C. A., Sosnick, T. R., and Pan, T. (2001) *RNA* 7, 233–241.
18. Hansen, A., Pfeiffer, T., Zuleeg, T., Limmer, S., Ciesiolka, J., Feltens, R., and Hartmann, R. K. (2001) *Mol. Microbiol.* 41, 131–143.
19. Loria, A., and Pan, T. (2001) *Nucleic Acids Res.* 29, 1892–1897.
20. Rox, C., Feltens, R., Pfeiffer, T., and Hartmann, R. K. (2002) *J. Mol. Biol.* 315, 551–560.
21. Pan, T. (1995) *Biochemistry* 34, 902–909.
22. Loria, A., and Pan, T. (1996) *RNA* 2, 551–563.
23. Massire, C., Jaeger, L., and Westhof, E. (1998) *J. Mol. Biol.* 279, 773–793.
24. Milligan, J. F., and Uhlenbeck, O. C. (1989) *Methods Enzymol.* 180, 51–62.
25. Seifert, S., Winans, R. E., Tiede, D. M., and Thiagarajan, P. (2000) *J. Appl. Crystallogr.* 33, 782–784.
26. Celander, D. W., and Cech, T. R. (1991) *Science* 251, 401–407.
27. Vioque, A., Arnez, J., and Altman, S. (1988) *J. Mol. Biol.* 202, 835–848.
28. Kunst, F., Ogasawara, N., Moszer, I., Albertini, A. M., Alloni, G., Azevedo, V., Bertero, M. G., Bessieres, P., Bolotin, A., Borchert, S., Borriss, R., Boursier, L., Brans, A., Braun, M., Brignell, S. C., Bron, S., Brouillet, S., Bruschi, C. V., Caldwell, B., Capuano, V., Carter, N. M., Choi, S. K., Codani, J. J., Connerton, I. F., Danchin, A., et al. (1997) *Nature* 390, 249–256.
29. Reich, C., Gardiner, K. J., Olsen, G. J., Pace, B., Marsh, T. L., and Pace, N. R. (1986) *J. Biol. Chem.* 261, 7888–7893.
30. Lewis, P. J., Thaker, S. D., and Errington, J. (2000) *EMBO J.* 19, 710–718.
31. Li, Z., and Deutscher, M. P. (2002) *RNA* 8, 97–109.
32. Ow, M. C., and Kushner, S. R. (2002) *Genes Dev.* 16, 1102–1115.

BI020416K